Al Azhar Bulletin of Science Vol. 30, No. 1, (June) 2019, pp. 35-45

PHOTODECONTAMINATION OF VAT GREEN 1 AND DIANIX BLUE DYES BY MWCNTs/x%TiO_2 NANOCOMPOSITES SYNTHESIZED USING EVAPORATION METHOD.

Badr A. El-sayed[a,*] , Walied A. A. Mohamed[b], Hoda R. Galal[b], H. M. H. Abd El-Bary[a], Mahmoud A.M. Ahmed[a]

[a] *Department of Chemistry, Faculty of Science, Al-Azhar University, Nasr City, Cairo, Egypt.*
[b] *Department of Inorganic Chemistry, National Research Centre, Giza, Egypt.*

ABSTRACT

Multi-walled carbon nanotubes (MWCNTs) were prepared using chemical vapour deposition (CVD) method. MWCNTs/titanium dioxide nanocomposites (MWCNTs/x%TiO_2) with different weight ratios of TiO_2 (x = 3, 6 and 10%) were synthesized using a simple modified evaporation method and used as a photocatalysts. Their photocatalytic activity investigated by studying the decontamination of two local textile dyes (Vat Green 1 and Dianix Blue Dyes) as an industrial organic pollutants commonly used in dyeing factories. The structure of the synthesized photocatalysts were characterized using XRD, SEM, diffused reflectance UV-Vis spectroscopic and N_2 adsorption-desorption method. Also, their optical band gaps were estimated, by Kubelka-Munk equation, as 3.51, 2.89, 2.80, 2.69 eV for MWCNTs and MWCNTs/x%TiO_2 respectively. The mineralization of Vat Green 1 and Dianix Blue dyes in presence of MWCNTs and MWCNTs/x%TiO_2 nanocomposites were investigated by determining the decrease in chemical oxygen demand (COD). In addition, the suggested possible mechanism of the photodegradation processes was studied.

Keywords: MWCNTs/%TiO_2 Nanocomposites, Evaporation Method, Photodegradation Process, Vat Green 1 Dye and Dianix Blue Dye.

1. INTRODUCTION

A novel one-dimensional (1D) carbon nanotubes (CNTs) have a specific character, unique mechanical properties and promising potential applications [1-7]. The uniformity in diameter, the dearth of purity, chirality and alignment has hindered searching of the intrinsic properties such as electronic, mechanical, sorption properties of CNTs in addition to their applications in novel electronic systems [8-12]. In last decades, various researches have been devoted to study the structure of CNTs and their high level surface area, stability toward electrochemical processes, thermal and electrical properties. CNTs have been used in removing hazardous pollutants from wastewater in industrial field such as leather and textile [13]. Due to its effectiveness, ideally producing nontoxic end products and easy operation, photocatalysis has been commonly used as a technique for the removing of industrial hazardous pollutants. TiO_2 (anatase) as a semiconductor with direct band gap of 3.18 eV (wavelength, lower than 388 nm), has been used as an active photocatalyst. The quick recombination problem of photogenerated charge carriers (electron-hole pairs) reduces the quantum efficiency of the photocatalytic process. Therefore, in recent years, many authors have been designed and developed nanocomposites including TiO_2 to avoid this problem and the pairing effect of MWCNTs with TiO_2 has been presented to provide a synergistic effect which can enhance the overall reaction of the dyes photodegradation [14-20], also TiO_2 can combined with other materials to like multi-nano walled carbon nanotubes to obtain good performance as photocatalyst. The prepared nanocomposites were evaluated for the photodegradation of the Vat Green 1 and Dianix Blue Dyes under Sunlight, UV and Xenon sources as well as the degree of complete degradation of the two dyes were assessed.

2. EXPERIMENTAL

2.1. Materials

Dianix Blue Dye (4,8-diamino-1,5-dihydroxy-2-(4-hydroxyphenyl)-4a,9a-dihydr-oanthracene-9,10-dione) molecular weight 362.34 g/mol and the molecular formula $C_{20}H_{14}N_2O_5$ and Vat Green 1 Dye (Anthra[9,1,2-cde] benzo[rst]pentaphene-5,10-dione, 16,17-dimethoxy) with molecular weight of 516.54 g/mol and the molecular formula is $C_{36}H_{20}O_4$, both of these local dyes used in dyeing process in Egypt. Sulphuric acid (H_2SO_4) 3M, nitric acid (HNO_3) 2M, Degussa P25 TiO_2 (78% :22% anatase :rutile) and deionized water. All chemicals purchased from Merck and SCRC, China, also all chemical reagents used without further purification and from analytical grade.

2.2. Measurements techniques

2.2.1. Scanning electron microscopy (SEM)

SEM of MWCNTs and MWCNTs/x%TiO_2 nanocomposites were observed using Philips XL-30 SEM analyzer (JEOL – JSM – T330 A) with an acceleration voltage 30 KV instrument.

2.2.2. X-ray diffraction (XRD)

X-ray diffraction were recorded by Philips Holland. Xpert MPD model using Cu-Kα target. (Cu Kα radiation = 0.154 nm, 40 mA, 50 kV; data recorded at a 0.017° step size and 100 s/step).

2.2.3. UV-Vis spectrophotometers

UV-Vis spectroscopy (Schimadzu) was conducted to monitor the concentration of the investigated dyes after photodegradation .

2.2.4. Chemical Oxygen Demand (COD)

The chemical oxygen demand COD is based on the chemical decomposition of compounds, dissolved or suspended in water by using COD Hanna Professional Instrument.

2.2.5. Photoreactors

The experimental setup was employed for the photocatalytic studies by using both of photoreactors UV-lamp (80-W) and Xe-lamp (50-W) (Eng. Co., Ltd., Egypt). Sunlight intensity for our experimental work was 3.4 lux for UV light and 1009 lux for visible light, which was measured by using (Lx-102 light meter).

2.3. Synthesis of MWCNTs and MWCNTs/x%TiO_2 nanocomposites

2.3.1. Synthesis of MWCNTs

MWCNTs were synthesized according to the literatures with some modification [21]. In present paper, MWCNTs were prepared by CVD method. The reactants were vaporized into a hydrogen/argon atmosphere at 720°C The MWCNTs as well as residual iron catalyst particles were removed by annealing the as-grown multi-walled carbon nanotubes in argon at 1760°C for 5 h. The production yield of MWCNTs in the converted carbon reaches 96%. To activate the surface, 1 gm of the prepared MWCNTs was dispersed in a mixture of concentrated acids of HNO_3 and H_2SO_4 with ratio of 1:3. The suspension kept in ultrasonic for 7 hr, then washed and dried at 100°C.

2.3.2. Synthesis of MWCNTs/x%TiO_2 nanocomposites

MWCNTs/x%TiO_2 nanocomposites were prepared using a simple modified evaporation method as follow. MWCNTs were dispersed in a 200 mL of H_2O and sonicated for 25 min. Then TiO_2 powder with different ratios of 1, 3, 6 and 10% was added to MWCNTs suspension during sonication. The suspension was filtered by using a vacuum evaporator to accelerate the water evaporation rate at 45°C. Then, the MWCNTs/x%TiO_2 composite were dried at 105°C for 24 h to avoid any probability of physicochemical changes in the carbon materials may occurs in the presence of oxygen at higher temperatures.

2.4. Photocatalytic processes

The photocatalytic processes of Vat green 1 and Dianix blue dyes were carried out using different light sources such as Sunlight, UV and Xenon irradiation without photocatalysts, and with MWCNTs, MWCNTs/3%TiO_2-MWCNTs/6%TiO_2-MWCNTs/10%TiO_2 nano-composites for various irradiation times to identify the economical and suitable process for

complete mineralization of the two textile dyes. The substrate concentration and the photocatalytic degradation experiments were studied to optimize the photocatalyst concentrations. Dianix Blue dye concentrations were varied from 2.8×10^{-5} M to 2×10^{-5} M and Vat Green 1 dye concentrations were varied from 2.2×10^{-5} M to 1.6×10^{-5} M. The photocatalyst concentrations were 0.1g/100 ml for all photocatalytic processes. On the other hand the photocatalytic degradation irradiation time was reached to 7 h. The photocatalyst concentration effect was studied by different the amounts of MWCNTs/%TiO_2 nanocomposites under irradiation with Sunlight, UV and Xenon lamps. The experimental setups were employed for the photocatalytic studies by using both of photoreactors UV-lamp (80-W) and Xe-lamp (50-W) (Eng. Co., Ltd., Egypt) and sunlight intensity was 3.4 lux for UV light and 1009 lux for visible light measured by (Lx-102 light meter). The concentration of the investigated dyes after photodegradation were analyzed by using a UV-Vis spectrophotometer (Schimadzu) by measuring the change in their maximum absorbance values at 623 nm for Dianix Blue dye and at 630 nm for Vat Green 1 dye. Also COD analysis used to confirm the mineralization of the two dyes.

3. RESULTS AND DISCUSSION

3.1. Characterizations And Measurements

3.1.1. XRD patterns of MWCNTs and MWCNTs/x%TiO_2 nanocomposites

The characteristic peaks around 25.7° and 41.9° appeared in XRD patterns as shown in (Figure - 1 (a)) were correspond to the (002) and (100) planes respectively reflected on the prepared MWCNTs**.** On the other hand the characteristic peaks observed in XRD patterns for MWCNTs/x%TiO_2 nanocomposites as shown in (Figure - 1 (b), (c) and (d)) located at 2Θ = 25.17°,36.48°,48.84°,54.66° and 62.37°, correspond to the (101), (004), (200), (211) and (204) planes respectively reflected on the prepared MWCNTs/x%TiO_2 nanocomposites. The shifts of the peaks are a result for trapping of electrons at the active sites of the nanocomposites, which results in hindering electron-hole pair recombination [22,23].

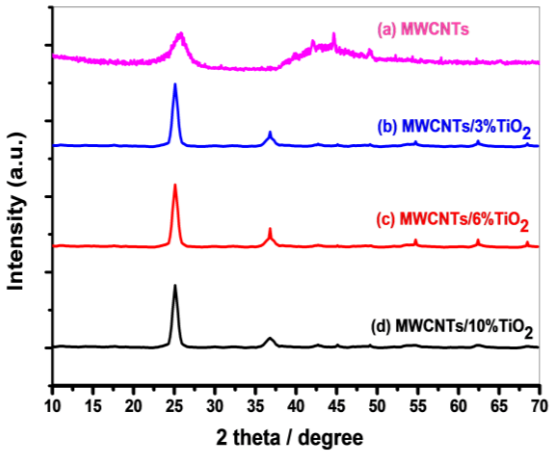

Figure (1) XRD patterns of the synthesized MWCNTs and MWCNTs/x%TiO_2 nanocomposites.

3.1.2. SEM of MWCNTs and MWCNTs/x%TiO_2 nanocomposites

The surface morphologies of the synthesized MWCNTs and MWCNTs/x%TiO_2 nano-composites were measured by SEM as shown in (Figure - 2). It explains the different morphology between the synthesized samples and indicates that the MWCNTs/x%TiO_2 nanocomposites present a homogeneous distribution of TiO_2 on the MWCNTs surface and less agglomeration of TiO_2 particles on MWCNTs surface, that suggesting a strong inter phase structure effect between TiO_2 and MWCNTs. So as to increase the surface area of the nanocomposites, so it was considered that MWCNTs/x%TiO_2 nanocomposites could perform much more activity and show a high photocatalytic activity. The patterns demonstrate the highly crystalline nature of the nanocomposites. And the surfaces of TiO_2 modified with MWCNTs are rough and little TiO_2 particles were dispersed on the MWCNTs which enhancing the photocatalytic activity for the synthesized nanocomposite.

3.1.3. Optical band gaps of MWCNTs and MWCNTs/x%TiO_2 nanocomposites.

The optical energy band gap of MWCNTs and its composites was determined using UV-Vis diffuse reflectance spectroscopy in Kubelka-Munk units. For a semiconductor materials, the investigation of optical absorption is considered as an appropriate

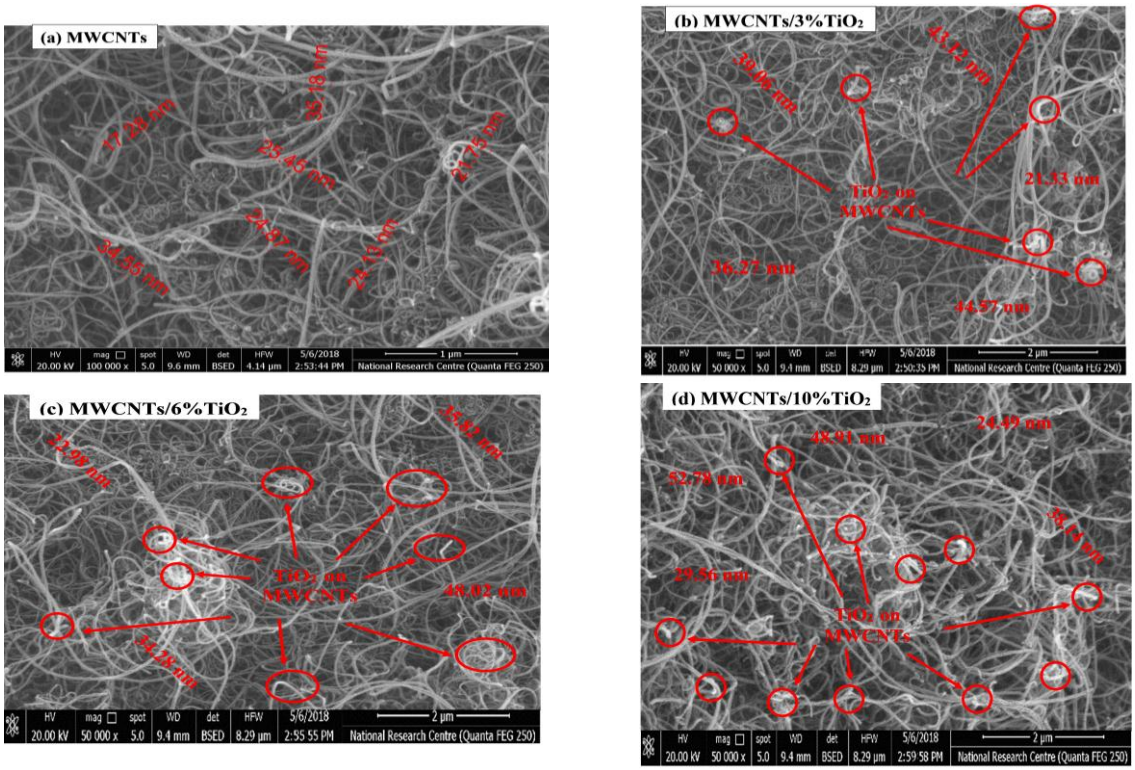

Figure (2) SEM images of the prepared MWCNTs and MWCNTs/x%TiO_2 nanocomposites

method for calculation of the optical band gaps and determining the kinds of transitions. The diffuse reflectance (R) converted into equivalent absorption coefficient F(R) (equation 1) [24].

$$F(R) = \frac{(1-R)^2}{2R} \quad (1)$$

This equation may be written as:

$$\left(\frac{(1-R)^2}{2R} x E\right)^{\frac{1}{n}} = (F(R) \times E)^{\frac{1}{n}} \quad (2)$$

Where (E) energy of light, n = ½ and 2 for direct and indirect allowed transitions, respectively, which characterizes the transition process, thus giving direct and indirect band gaps. The band gap for the photocatalysts may be determined from the plot of $(F(R) \times E)^{\frac{1}{n}}$ versus energy of light (E) measured in eV from the intersection of the tangent via inflection point in absorption band and the photon energy axis. Band gap energy was calculated using Tauc equation (see equation 3):

$$(\alpha h\nu)^{\frac{1}{n}} = B(h\nu - E_g) \quad (3)$$

Which may be written as :

$$(F(R) \times E)^{\frac{1}{n}} = B(h\nu - E_g) \quad (4)$$

where n = ½ and 2 for direct and indirect transitions, respectively, α is (absorption coefficient), ν is (light frequency), h is (a Planck constant), B is (a constant independent on photon energy but depends on the transition probability) and the optical band gap (E_g) The band gap energy for the synthesized samples may also be measured by the same method from the plot of $(\alpha h\nu)^{\frac{1}{n}}$ versus (hν) energy of light, this also depended on the intersection of the tangent via inflection point in absorption band and the photon energy axis as shown in (figure - 3). Where for allowing direct transitions, where, n= ½, equation (3) becomes:

$$(\alpha h\nu)^2 = B(h\nu - E_g) \quad (5)$$

Table (1) Band gap of MWCNTs and MWCNTs/x%TiO_2 nanocomposites samples

Photocatalyst	band gap (eV)
MWCNTs	3.51
MWCNTs/3%TiO_2	2.89
MWCNTs/6%TiO_2	2.80
MWCNTs/10%TiO_2	2.69

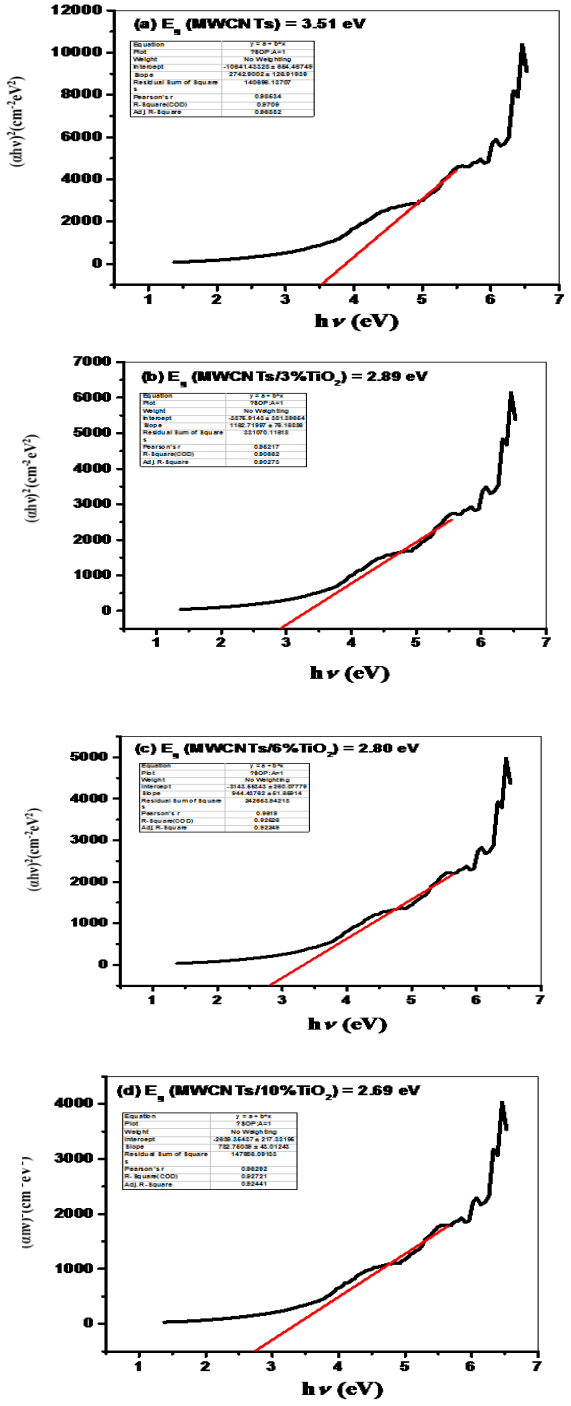

Figure (3) Kubelka-Munk curves for band gap estimation of)a) MWCNTs and (b, c and d) MWCNTs with different TiO_2 % (3, 6 and 10%), respectively.

The optical band gap energy (E_g) calculated values are shown in Table-1. The value of E_g for MWCNTs was 3.51 eV, which decreases to 2.89, 2.80 and 2.69 eV for MWCNTs/3%TiO_2, MWCNTs/6%TiO_2 and MWCNTs/10%TiO_2 respectively. This effect may be due to two reasons, an increase in vacancies or chemical defects present in the intergranular areas, also due to the chemical interaction between MWCNTs and TiO_2 to create a new energy level reducing the E_g. MWCNTs/x%TiO_2 nanocomposites with less E_g are optically active and used in photocatalytic degradation for environmental decontamination. The decrease in band gap values suggests high photocatalytic activity of the synthesized nanocomposites in visible light range. From the obtained values, it is clear that the band gap values depend on both MWCNTs support and the TiO_2 percentages in the binary nanocomposites. The variation of the band gap with increasing the particle size is an important role for photocatalytic activity of MWCNTs/x%TiO_2 nanocomposites [25-27]. The functionalization of MWCNTs and TiO_2 is expected to enhance the efficiency of the photocatalytic activity of the produced nanocomposites.

3.1.4. BET of MWCNTs and MWCNTs/x%TiO_2 nanocomposites

Table-2 presents the surface area Brunauer-Emmett-Teller (BET) (m^2/g), total pore volume (cm^3/g), average pore diameter (nm) and monolayer adsorption amount (V_m) of the MWCNTs and synthesized MWCNTs/x%TiO_2 nanocomposites. The surface area of MWCNTs, MWCNTs/3%TiO_2, MWCNTs/ 6%TiO_2 and MWCNTs/10%TiO_2 are 95.201, 98.142, 104.251 and 117.125 m^2/g respectively (see Table-2).

Table (2) BET parameters of MWCNTs and MWCNTs/x%TiO_2 nanocomposites samples

Photocatalyst	MWCNTs	MWCNTs/3%TiO_2	MWCNTs/6%TiO_2	MWCNTs/10%TiO_2
BET (m^2/g)	95.201	98.142	104.251	117.125
Total pore volume (cm^3/g)	0.2139	0.2089	0.2001	0.1939
Average pore diameter (nm)	8.987	9.181	9.301	9.521
V_m (cm^3/g)	21.843	22.148	22.800	23.113

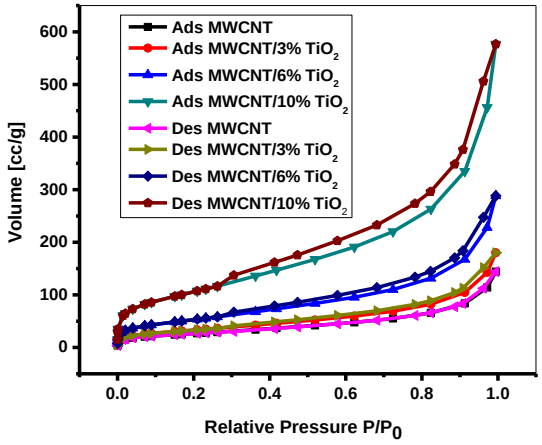

Figure (4) Nitrogen adsorption-desorption for all photocatalysts.

All the photocatalysts represent type IV curves showing a typical hysteresis loop associated with capillary condensation of gases within mesopores (Figure 4) [28]. Such mesoporous photocatalysts structure provides efficient transport pathways to the interior, which may be useful for improving the photocatalytic activity. With a further increase in the amount of TiO_2, however, this peak broadens and increases. This phenomenon indicates that correlation between TiO_2 loading and pore size distributions of synthesized MWCNTs/x%TiO_2 nanocomposites. Also, the adsorption isotherms shifts upwards and the hysteresis loop moves to low pressure range. From pore size distribution results for all samples, it observed that MWCNTs with smallest average pore diameter have also the smallest surface area while by increasing amount of TiO_2 surface area increases refers to their average pore diameter increasing as shown in Table-2. From the above results, the band gap decreasing in presence of TiO_2 and decreases as their amount increases is due to the accelerate in the mass transfer and generating the more reaction sites which led to enhancing in the photocatalytic process.

3.2. Photocatalytic activity of MWCNTs and MWCNTs/x%TiO_2

3.2.1. Effect of the initial dye concentration

The maximum absorption peaks of Vat Green 1 dye and Dianix Blue dye were located at 630 and 623 nm respectively. From the following Figure, 2.6×10^{-5} M and 2×10^{-5} M were the suitable concentrations for the photodegradation processes for the two dyes (a) Dianix Blue and (b) Vat Green 1, respectively.

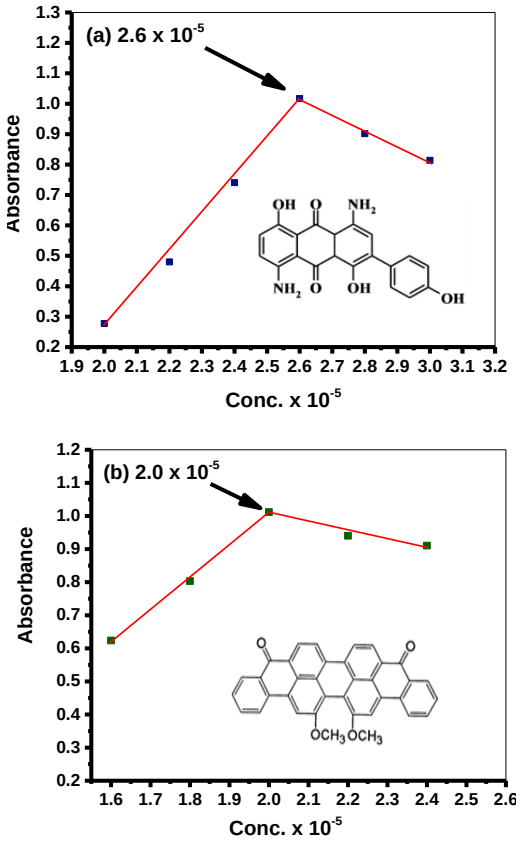

Figure (5) Effect of initial concentration of (a) Dianix Blue and (b) Vat Green 1 dyes

3.2.2. Photocatalytic degradation of Vat Green 1 and Dianix Blue 1 dyes

The photocatalytic degradation rates of the two dyes Vat Green 1 and Dianix Blue using Sunlight, UV and Xenon irradiation was monitoring spectrophotometrically in UV–Vis range as shown in Figure - 6, according to equation (6).

$$\ln(\frac{C_o}{C}) = k_{app}\, t \qquad (6)$$

where C is the concentration at time t, C_0 is the initial concentration of the dye and k_{app} is the apparent reaction rate constant of the photodegradation process. From Figure-6 a linear relationship was obtained between $\ln(\frac{C_o}{C})$ and irradiation time. The

photocatalytic experiments of the two dyes follow the pseudo first order kinetics. Three sets of experiments for each dye were performed using three types of light sources (Sunlight, UV and Xenon) respectively to observe the adsorption and photocatalytic effects of MWCNTs and the synthesized nanocomposites. It was noted that the BET surface area of MWCNTs, MWCNTs/3%TiO_2, MWCNTs/6%TiO_2, and MWCNTs/10%TiO_2 are 95.201, 98.142, 104.251 and 117.125 m^2/g respectively (see Table-2). Table 3 shows the photocatalytic reaction rate constants (k_{app}), the synergy factors (R) and COD) values. Comparing the k_{app} for all photodegradation processes of the dyes using MWCNTs, MWCNTs/3%TiO_2, MWCNTs/6%TiO_2, MWCNTs/10%TiO_2 photocatalysts. The photodegradation rate increases greatly in the existence of MWCNTs/x%TiO_2 nanocomposites and in the order of MWCNTs/10%TiO_2 > MWCNTs/6%TiO_2 > MWCNTs/3%TiO_2 > MWCNTs. Hence the surface area increases as 95.201, 98.142, 104.251 and 117.125 m^2/g for MWCNTs, MWCNTs/3%TiO_2, MWCNTs/6%TiO_2 and MWCNTs/10%TiO_2 respectively (see Table-2). As expected when TiO_2 is exposed to photons and the electrons are transfer from valence band to conduction band resulting in the formation of equal numbers of holes in the valence band, as in (equation 7).

$$TiO_2 + h\nu \rightarrow h^+ + e^- \quad (7)$$

Then $$e^- + O_2 \rightarrow O_2^{\cdot -} \quad (8)$$

On the other hand, $$H_2O + h^+ \rightarrow H^+ + {}^{\cdot}OH \quad (9)$$

$$OH^- + h^+ \rightarrow {}^{\cdot}OH \quad (10)$$

The generated hydroxyl radicals attack the organic dyes adsorbed onto the photocatalyst surface in solution and oxidized them [29,30] as shown in Figure 7.

The synergy factor (R) is expressed as in equation (11).

$$R = \frac{k_{app\left(\frac{MWCNTs}{x}\%TiO2\right)}}{k_{app\,(MWCNTs)}} \quad (11)$$

Where $k_{app\,(MWCNTs)}$ and $k_{app\left(\frac{MWCNTs}{x}\%TiO2\right)}$ refers to the apparent rate constant for the photocatalytic activity of MWCNTs and the synthesized nanocomposites respectively.

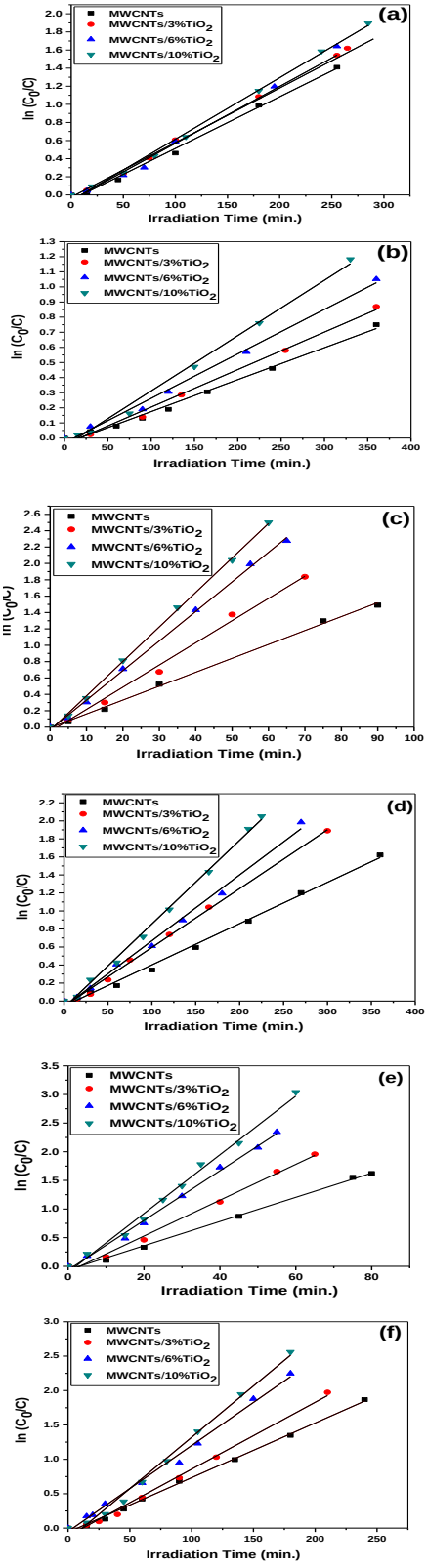

Figure (6) Pseudo first order linear plots of ln (C_0/C) vs. irradiation time for the degradation kinetics of Dianix Blue dye (a, c and e) and Vat Green 1 dye (b, d and f) under different Sunlight, UV and Xenon irradiation, respectively.

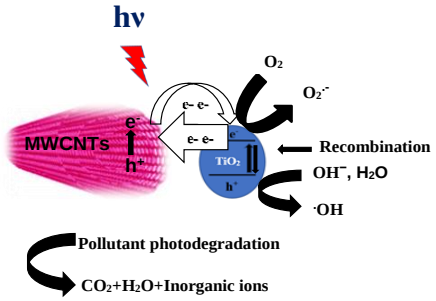

Figure (7) Schematic diagram of the proposed mechanism of photocatalytic degradation over MWCNTs /TiO_2 nanocomposite.

Generally, the organic pollutant dyes can't degrade completely under Sunlight irradiation and according to Egyptian Environmental Law (Law NO.9) [31,32], The COD value allowed is less than 1000 ppm. From the above table, the photodegradation of the two dyes in presence of MWCNTs and MWCNTs/x%TiO_2 nanocomposites under Sunlight still had COD (ppm) values higher than the allowed value (1000 ppm). While the photodegradation of the two dyes exposed to both of UV and Xenon light sources recorded COD values less than 1000 (ppm), especially the MWCNTs/10%TiO_2 samples which has COD values less than 1000 (ppm), this indicate that they are used as excellent photocatalysts. Table-3 indicated that the photocatalytic degradation process of the dyes increases with increasing the TiO_2 weight percent in the nanocomposites from 3 to 10% and reaches its maximum at a 10%TiO_2 in the nanocomposite. Also the highest photodegradation rate was observed using Xenon irradiation with MWCNTs/10%TiO_2 nanocomposite, where the number of photons absorbed and the number of dye molecules adsorbed on the photocatalysts were increased which promotes the photodegradation rate.

Table (3) Photodegradation rates (k_{app}), synergy factors (R) and Chemical Oxygen Demand (COD) values of the two dyes with different photocatalysts in the existence of different irradiation sources.

Sunlight irradiation	Dianix Blue dye			
	Photocatalyst	k_{app} (s^{-1})	R	COD (ppm)
	MWCNTs	0.00571 ± 1.95619E-4	1	2645
	MWCNTs/3%TiO_2	0.00622 ± 9.45456E-5	1.089	2470
	MWCNTs/6%TiO_2	0.00658 ± 2.44397E-4	1.152	2108
	MWCNTs/10%TiO_2	0.00679 ± 1.52953E-4	1.189	1985
	Vat Green 1 dye			
	Photocatalyst	k_{app} (s^{-1})	R	COD (ppm)
	MWCNTs	0.00212 ± 7.95952E-5	1	3785
	MWCNTs/3%TiO_2	0.00248 ± 1.03928E-4	1.169	3205
	MWCNTs/6%TiO_2	0.00294 ± 1.11411E-4	1.386	2988
	MWCNTs/10%TiO_2	0.00366 ± 1.36129E-4	1.726	2645
UV irradiation	Dianix Blue dye			
	Photocatalyst	k_{app} (s^{-1})	R	COD (ppm)
	MWCNTs	0.017 ± 3.50919E-4	1	2258
	MWCNTs/3%TiO_2	0.02711 ± 0.00111	1.594	1310
	MWCNTs/6%TiO_2	0.03612 ± 5.76817E-4	2.124	1025
	MWCNTs/10%TiO_2	0.04213 ± 5.54871E-4	2.478	865
	Vat Green 1 dye			
	Photocatalyst	k_{app} (s^{-1})	R	COD (ppm)
	MWCNTs	0.00458 ± 1.21127E-4	1	2185
	MWCNTs/3%TiO_2	0.00653 ± 1.52995E-4	1.425	1764
	MWCNTs/6%TiO_2	0.00732 ± 2.23643E-4	1.598	1388
	MWCNTs/10%TiO_2	0.00929 ± 1.99737E-4	2.028	925
Xenon irradiation	Dianix Blue dye			
	Photocatalyst	k_{app} (s^{-1})	R	COD (ppm)
	MWCNTs	0.02114 ± 5.88147E-4	1	2101
	MWCNTs/3%TiO_2	0.03128 ± 0.00119	1.479	1156
	MWCNTs/6%TiO_2	0.04332 ± 0.00114	2.049	864
	MWCNTs/10%TiO_2	0.05126 ± 0.00168	2.424	714
	Vat Green 1 dye			
	Photocatalyst	k_{app} (s^{-1})	R	COD (ppm)
	MWCNTs	0.00795 ± 1.53579E-4	1	1785
	MWCNTs/3%TiO_2	0.00973 ± 3.45827E-4	1.223	1325
	MWCNTs/6%TiO_2	0.01251 ± 3.55707E-4	1.573	1080
	MWCNTs/10%TiO_2	0.01491 ± 5.29326E-4	1.875	897

CONCLUSION

Semiconductor photocatalysis seems to be a promising technology that encompasses a range of applications in environmental systems such as hazardous waste remediation, air purification. Photocatalytic oxidation using MWCNTs, MWCNTs/3%TiO_2, MWCNTs/ 6%TiO_2 and MWCNTs/10%TiO_2 nano-composites in the presence of Sunlight, UV and Xenon lights were effectively applied for the photodegradation of Vat Green 1 and Dianix Blue dyes. Also, the percentage of TiO_2 in nanocomposites has a synergistic effect on MWCNTs, polymorphs of TiO_2 due to the dominant structure which cause high levels of crystalline of the nanocomposites. So it concluded that the synthesized nanocomposites have a good photocatalytic activity especially the MWCNTs/10%TiO_2 sample. Both of the photodegradation rates k (s^{-1}) and the synergy factors (R) were increased, also the photodegradation processes using COD analysis revealed a higher degree of complete mineralization of the two textile dyes especially by using Xenon irradiation, so these nanocomposites were an effective for the removal of the dyes from an aqueous solution and follow COD limits of Egyptian Environmental Law (Law NO.9).

REFERENCES

1. A. M. Kamil, H. T. Mohammed, A. A. Balakit, F. H. Hussein, D. W. Bahnemann, and G. A. El-Hiti, "Synthesis, Characterization and Photocatalytic Activity of Carbon Nanotube/Titanium Dioxide Nanocomposites" *Arab. J. Sci. Eng*., vol. 43, No. 1, pp. 199-210, 2018.
2. Y. Huang, R. Li, D. Chen, X. Hu, P. Chen, Z. Chen, and D. Li, "Synthesis and Characterization of CNT/TiO_2/ZnO Composites with High Photocatalytic Performance" *Catalysts*, vol. 8, No. 4, pp. 151-156, 2018.
3. J. O. Marques Neto, C. R. Bellato, C. H. F. De Souza, R. C. Da Silva, and P. A. Rocha, "Synthesis, Characterization and Enhanced Photocatalytic Activity of Iron Oxide/Carbon Nanotube/Ag-doped TiO_2 Nanocomposites"*J. Braz. Chem. Soc.*, vol. 28, No. 12, pp. 2301-2312 ,2017.
4. N. M. Mahmoodi, P. Rezaei, C. Ghotbei, and M. Kazemeini, Fibers, "Copper oxide-carbon nanotube (CuO/CNT) nanocomposite: Synthesis and photocatalytic dye degradation from colored textile wastewater" *Polym*., vol. 17, No. 11, pp. 1842-1848 , 2016.
5. M. Shaban, A. M. Ashraf, and M. R. Abukhadra, "TiO2 Nanoribbons/Carbon Nanotubes Composite with Enhanced Photocatalytic Activity; Fabrication, Characterization, and Application" *Characterization, and Application. Sci. Rep*., vol. 8, No. 781, 1-17, 2018.
6. A. Salama, A. Mohamed, N. M. Aboamera, T. A. Osman, and A. Khattab, "Photocatalytic degradation of organic dyes using composite nanofibers under UV irradiation"*Appl. Nanosci*., vol. 8, pp. 155-161 , 2018.
7. A. Mohamed, S. Yousef, M. Ali Abdelnaby, T.A. Osman, B. Hamawandi, M.S. Topark, M. Muhammed and A. Uheida, "Photocatalytic degradation of organic dyes and enhanced mechanical properties of PAN/CNTs composite nanofibers"*Sep. Purif. Technol*., vol. 182, pp. 219-223, 2017.
8. W. Zhu, Z. Li, C. He, S. Faqian and Y. Zhou, "Enhanced photodegradation of sulfa-methoxazole by a novel WO_3-CNT composite under visible light irradiation" *J. Alloys Compd.*, vol. 754, pp. 153-162, 2018.
9. R. S. Lankone, J. Wang, J. F. Ranville, and D. H. Fairbrother, "Photodegradation of polymer-CNT nanocomposites: effect of CNT loading and CNT release characteristics"*Environmental Science: Nano*, vol. 4, 967-982, 2017.
10. W. Yang, L. Lang, X. Yin, and C. Wu, "Formation mechanism of 0.4-nm single-walled carbon nanotubes in $AlPO_4$-5 crystals by low-temperature hydrocracking" *Carbon*, vol. 115, pp. 120-127, 2017.
11. D. Eder, "Carbon Nanotube−Inorganic Hybrids" *Chem. Rev*., vol. 110, pp. 1348-1385, 2010.
12. J. Moma, J. Baloyi, and T. Ntho, "Synthesis and characterization of an efficient and stable Al/Fe pillared clay catalyst for the catalytic wet air oxidation of phenol"*RSC Adv.*, vol. 8, pp. 30115-30124, 2018.
13. M. Loginov, N. Lebovka, and E. Vorobiev, "Hybrid Multiwalled Carbon Nanotube − Laponite Sorbent for Removal of Methylene Blue from Aqueous Solutions*" Journal of Colloid and Interface Science*, vol. 431, pp. 241-249, 2014.

14. D. M. El-Mekkawi, A. A. Labib, H. A. Mousa, H. R. Galal, and W. A. A. Mohamed, "Preparation and Characterization of Nano Titanium Dioxide Photocatalysts Via Sol Gel Method over Narrow Ranges of Varying Parameters" *Orient. J. Chem.*, vol. 33, No. 1, pp. 41-51, 2017.

15. A. Aliyu, A. Abdulkareem, A. Kovo, O. Abubakre, J. Tijani, and I. Kariim, "Synthesize multi-walled carbon nanotubes via catalytic chemical vapour deposition method on Fe-Ni bimetallic catalyst supported on kaolin" *Carbon Letters*, vol. 21, No. 33, pp. 33-50, 2017.

16. G. Ma, Y. Zhu, Z. Zhang, and L. Li, "Preparation and characterization of multi-walled carbon nanotube/TiO"2 composites: Decontamination organic pollutant in water" *Appl. Surf. Sci*., vol. 313, pp. 817-822, 2014.

17. A. M. Kamil, F. H. Hussein, A. F. Halbus, and D. W. Bahnemann, "Preparation, Characterization, and Photocatalytic Applications of MWCNTs/TiO_2 Composite" *International Journal of Photoenergy*, vol. 2014, No. 1, pp. 1-8, 2014.

18. I. Ali, M. Suhail, Z. A. Alothman, and A. Alwarthan, "Recent advances in syntheses, properties and applications of TiO_2 nanostructures" *RSC Adv.*, vol. 8, pp. 30125-30147, 2018.

19. D. Heltina, P. P. D. K. Wulan, and Slamet, "Synthesis and Characterization of Titania Nanotube-Carbon Nanotube Composite for Degradation of Phenol" *Journal of Chemical Engineering*, vol. 6, pp. 1065-1068, 2015.

20. G. Rahman, Z. Najaf, A. Mehmood, S. Bilal, A. Shah, S. Mian, and G. Ali, "An Overview of the Recent Progress in the Synthesis and Applications of Carbon Nanotubes" *Journal of Carbon Research*, vol. 5, No. 1, pp. 1-31, 2019.

21. G. Allaedini, S. M. Tasirin, and P. Aminayi, "Synthesis of CNTs via chemical vapor deposition of carbon dioxide as a carbon source in the presence of NiMgO" *Journal of Alloys and Compounds*, vol. 647, pp. 809-814, 2015.

22. C. E. El shafiee, M. O. Abdel-salam, S. M. N. Moalla , H. R. Ali , D. I. Osman, R. I. Abdallah , and Y.M. Moustafa, "Carbon Nanotubes as Superior Sorbent for Removal of Phenol from Industrial Waste Water" *Egy. J. Chem*., vol. 61, No. 1, pp. 75-84, 2018.

23. A. Alwash, H. Adil, Z. Hussain, and E. Yousif, "Potential of Carbon Nanotubes in Enhance of Photocatalyst Activity" *Arch. Nanomedicine*, vol. 1, No. 3, pp. 65-70, 2018.

24. A. A. Ismail, A. M. Ali, F. A. Harraz, M. Faisal, H. Shoukry، and A. E. Al-Salami, "A Facile Synthesis of alpha-Fe2O3/Carbon Nanotubes and Their Photocatalytic and Electrochemical Sensing Performances" *Int. J. Electrochem. Sci.*, vol. 14, pp. 15-32, 2019.

25. M. Nowak, B. Kauch and P. Szperlich, "Determination of energy band gap of nanocrystalline SbSI using diffuse reflectance spectroscopy" *Rev. Sci. Instrum*., vol. 80, No. 4, pp. 1- 12, 2009.

26. M. Chandrakala, S. Raj Bharath, T. Maiyalagan and S. Arockiasamy, "Synthesis, crystal structure and vapour pressure studies of novel nickel complex as precursor for NiO coating by metalorganic chemical vapour deposition technique" *Mater. Chem. Phys*., vol. 201, pp. 344-353, 2017.

27. M. Thirumoorthi and J. T. J. Prakash, "Effect on the properties of ITO thin films in Gamma environment" J. Superlattices and Microstructures, vol. 85, pp. 237-247, 2015.

28. J. Yu, T. Ma, G. Liu and B. Cheng, "Enhanced photocatalytic activity of bimodal mesoporous titania powders by C_{60} modification" Dalt. Trans., vol. 40, pp. 6635-6644, 2011.

29. J. G. Yu, X. H. Zhao, H. Yang, X. H. Chen, Q. Yang, L. Y. Yu, J. H. Jiang, and X. Q. Chen, "Aqueous adsorption and removal of organic contaminants by carbon nanotubes" Science of the Total Environment, vol. 482, pp. 241-251, 2014.

30. E. F. A. Zeid, I. A. Ibrahem, A. M. Ali, and W. A. A. Mohamed, "The effect of CdO content on the crystal structure, surface morphology, optical properties and photocatalytic efficiency of p-NiO/n-CdOnanocomposite" Results Phys., vol. 12, pp. 562-570, (2019).

31. U.S. Environmental Protection Agency (EPA). (2008) EPA's 2008 Report on the Environment. National Center for Environmental Assessment, Washington, DC; EPA/600/R-07/045F, *http://www.epa.gov/roe*, 2008.

32. Affairs, E., Law Number 9 of 2009 on Investment. *http://www.eeaa.gov.eg/en-us/laws/envlaw.aspx*, 2009.

إزالة ضوئية لتلوثات صبغتي الڤات الخضراء ١ والديانيكس الزرقاء باستخدام أنابيب الكربون النانوية متعددة الجدران المطعمة بنسب وزنية من ثانى أكسيد التيتانيوم المركبة المحضرة باستخدام طريقة التبخر

[١]بدرالدين عواد السيد محمد، [٢]وليد عبدالحليم عبدالغفار محمد، [٢]هدى محمد رفعت محمد جلال،

[١]حسن محمد حسن عبدالباري، [١]محمود علي محمود احمد

[١]قسم الكيمياء - كلية العلوم (بنين) – جامعة الأزهر

[٢]قسم الكيمياء – المركز القومي للبحوث - الجيزة - مصر

الملخص العربى

دراسة نشاط التحفيز الضوئي لمركبات (الأنابيب النانوية الكربونية المتعددة الجدران/ ثاني أكسيد التيتانيوم النانوي) $MWCNTs/x\%TiO_2$ مع نسب أوزان مختلفة من TiO_2 (س = ٣ ، ٦ و ١٠ ٪) تم توليفها باستخدام طريقة تبخر معدلة بسيطة في إزالة التلوث من صبغتين محليتين من أصباغ النسيج وهما (Vat Green 1 و Dianix Blue) كملوثات عضوية صناعية شائعة الاستخدام في مصانع الصباغة. وقد تم توصيف بنية المركبات النانوية المحضرة MWCNTs و $MWCNTs/x\%TiO_2$ ذات المحفزات الضوئية بنسب مختلفة من الوزن باستخدام حيود الأشعة السينية ، الماسح الميكروسكوبي الإلكتروني ، تقنية التحليل الطيفي للأشعة فوق البنفسجية والمرئية المنعكسة ، وطريقة امتصاص N_2. كما تم تقدير فجوة النطاق البصري بواسطة معادلة Kubelka-Munk لـ MWCNTs و$MWCNTs/x\%TiO_2$ مما يعطي قيم ٣,٥١ و ٢,٨٩ و ٢,٨٠ و ٢,٦٩ إلكترون فولت على التوالي. تم قياس مقدار تحويل الصبغتين لعناصرهم الأساسية باستخدام عمليات قياس النقص في محتوى الأكسجين الكيميائي . بالإضافة إلى آلية محتملة تم اقتراحها لعمليات التحلل الضوئي لصبغتي الڤات الخضراء ١ والديانيكس الزرقاء في وجود الحافزات الضوئية المحضرة.